

EFFECTS OF TARGET PROPERTIES ON SEISMIC EFFICIENCY IN METER-SIZE CRATERS ON MARS. A. Rajšić¹, K. Miljković¹, G.S. Collins², K. Wünnemann³, M.A. Wieczorek⁴, N. Wójcicka² and I.J. Daubar⁵; ¹School of Earth and Planetary Science, Space Science and Technology Center, Curtin University, Perth, Australia; ²Imperial College London, UK; ³Museum für Naturkunde, Berlin, Germany; ⁴Université Côte d'Azur, Observatoire de la Côte d'Azur, CNRS, Laboratoire Lagrange, France; ⁵Brown University, Providence, RI, USA. (andrea.rajsic@postgrad.curtin.edu.au)

Introduction: For a year we have been receiving seismic data from the seismometer SEIS that was deployed on Mars by the NASA InSight Mission [1-3]. One of the expected sources of seismic is bombardment by small meteoroids [4-5]. During an impact, a small portion of the impact energy is transformed into seismic energy, and that energy ratio is called the seismic efficiency. Previous numerical impact investigations showed that target properties, such as porosity, can affect the pressure wave propagation and thus the seismic efficiency [4-8]. Here we numerically investigate how different strength and porosity models for Mars analogue materials affect the seismic efficiency estimates in small craters.

Seismic efficiency: Estimates of seismic efficiency range from $k=10^{-2}$ to 10^{-6} [5-9]. High seismic efficiency is typical in bedrock or highly consolidated materials ($k>10^{-3}$). Low seismic efficiency is typical for sediments or unconsolidated sands and soils ($k<10^{-5}$) [4;6-11]. In this work, we used a simplified approach [6-9] that defines the seismic efficiency as:

$$k = \frac{\pi x^2 P^2 \Delta t}{3 \rho C_p E_i}$$

where x represents distance from the impact point, P is the amplitude of the pressure pulse, t is the duration of the pressure pulse, ρ is the density of the target, C_p is the speed of sound in the target and E_i is the kinetic energy of the impactor.

Although this representation for the seismic efficiency is simplified, it can still be used to investigate the target effects, and how parameters that govern k change with respect to a chosen material model and impact conditions, specifically regolith vs. bedrock. Target properties were varied: cohesion of the target and porosity (0%, 10%, 37%, 44%, and 65%).

Numerical impact modelling: All simulations were made in the iSALE-2D shock physics hydrocode [12]. Impact energy was within the range of impact energies expected during the lifetime of the InSight mission (10^6 , 10^8 , 10^{10} , 10^{11} , 10^{12} J) [13].

In both models we used the Lundborg strength model (LUNDD) [14]. This is non-linear pressure-dependent strength model for damaged rock. We varied cohesion of the target. In first model cohesion was 10kPa and second model had cohesion set to 5 kPa (Table 1). The projectile material model in all cases

used the same strength model as the target, but without porosity.

Table 1. Varied strength model parameters

Parameter	Model 1	Model 2
Strength	LUNDD	LUNDD
Damage	NONE	NONE
Cohesion	10 KPa	5 KPa
Friction	0.7	0.7

We used the Tillotson equation of state for basalt [15-16]. For porous cases, we used the ϵ - α porosity model [17]. In this model, α_0 represents the initial distension, α_x represents distension at transition from exponential to power-law compaction; ϵ_0 is the elastic volumetric strain threshold, χ is the ration of speed of sound in porous vs non-porous case for the target material at zero pressure and c is the compaction rate parameter in the compaction regime [17]. The parameters were adopted from [18] (Table 2).

Table 2. Porosity model parameters

Porosity	α_0	α_x	ϵ_0	c	χ
10%	1.1	1.05	-0.01	0.98	0.9
37%	1.6	1.15	-0.01	0.98	0.33
44%	1.8	1.1	-0.01	0.98	0.33
65%	2.8	1.6	-0.01	0.97	0.21

All variables in the equation for the seismic efficiency were calculated in iSALE simulations. The pressure wave was observed via gauges cells, placed at 45° equidistantly throughout the target (Figure 1). The pressure wave amplitude and pulse duration were calculated at full width half maximum. The sound speed was assumed to be equal to the speed of the observed pressure wave.

Dependence on target porosity. Figure 1 shows pressure wave attenuation for the same strength model but different target porosities, for the same $E_i=4 \times 10^6$ J. Figure 1 illustrates how target porosity affects the speed of the pressure wave. The pressure wave captured at the same distance from the impact point in four targets of different porosities at different time stamps. It is noticeable that the wave speed depends on the properties of the target. The pressure wave needed 80% more time in the 65% porous target to reach the same distance then the wave traveling through the non-porous bedrock. This is a result of the loss of impact

energy during crushing and compacting of pore space in porous media, but also because the speed of sound is defined by the bulk modulus and density of the medium.

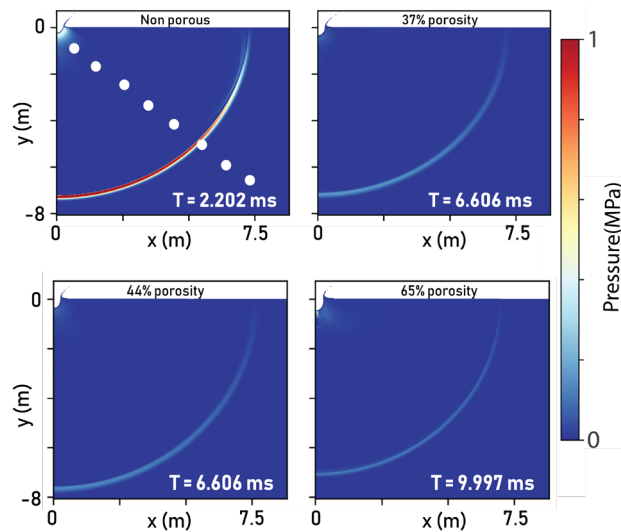


Figure 1. Impact simulations showing the pressure wave traveling through 0% (top left), 37% (top right), 44% (bottom left), and 65% (bottom right) target porosity.

Estimates for the seismic efficiency changed by almost an order of magnitude between bedrock and all the porous cases. For non-porous bedrock $k=1.66 \times 10^{-3}$ and for 10% porous regolith $k=8.08 \times 10^{-4}$. For 37% porous regolith $k=7.90 \times 10^{-4}$. For 44% and 65% porous regolith $k=2 \times 10^{-4}$. These results are consistent with the value of $k=5 \times 10^{-4}$ that was adopted for a generic Mars case [4]. Our numerical investigation helps constrain this estimate further.

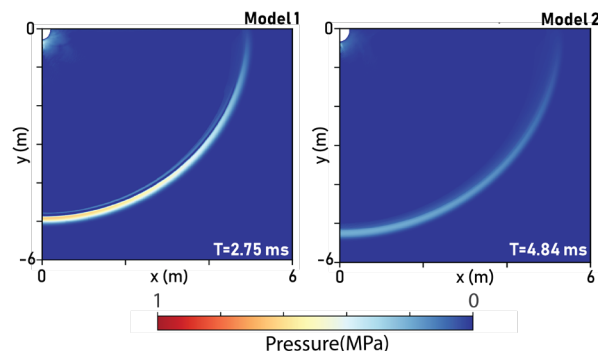


Figure 2. Impact simulations showing the pressure wave traveling through media with different strength models.

Dependence on strength models. We calculated seismic efficiencies for two scenarios (Models 1 and 2, Table 1). Porosity in the target was 44% in both mod-

els (Table 2). Figure 2 shows that at the same distance from the impact point, the peak pressure values were different. Between the models difference in value of the maximum pressure at the same distance from the impact point was 30%. This shows that lower cohesion in the same strength model slowed down pressure wave, hence peak pressure was lower for 30% in lower cohesion target model.

As a consequence of the pressure wave propagation being affected by different strength models, the resulting calculated seismic efficiency was also different. For Model 1, $k=2.00 \times 10^{-4}$, Model 2, $k=2.88 \times 10^{-4}$. Different strength models used for target properties affect pressure wave propagation but the estimates of the seismic efficiency remained within the same order magnitude.

Conclusion. The biggest differences in seismic efficiencies and wave propagation are between porous and non-porous cases. Differences between porous cases do exist but they are in the same order of magnitude. Different strength models used for target properties affect pressure wave propagation but the estimates of the seismic efficiency remained within the same order of magnitude. These results can help in better understanding of a) impact conditions and b) target properties, and they require further investigation.

Acknowledgments: We gratefully acknowledge the developers of iSALE (<https://isale-code.github.io/>). AR and KM are fully supported by the Australian Research Council (DP180100661 and DE180100584).

References: [1] Lognonne, P. *et al.* (2019) *Space Sci. Rev.*, 215:12. [2] Lognonne, P. *et al.* (2020) *Nature Geosci.*, accepted. [3] Giardini, D. *et al.* (2020) *Nature Geosci.*, accepted [4] Daubar I. *et al.* (2018) *Space Sci. Rev.*, 214(8). [5] Daubar, I. *et al.* (2020) LPI Contribution, this issue [6] GÜldemeister N. & Wünnemann K. (2017) *Icarus*, 296, 15–27. [7] Miljković K. *et al.* (2019) *LPSC LPI Contribution No. 1503*. [8] Wójcicka N. *et al.* (2019) *LPSC LPI Contribution No. 2633*. [9] Schultz P.H. & Gault D.E. (1975) *The Moon*, 12(2), 159-177. [10] Latham G. *et al.* (1970) *Science*, 170(3958), 620-626. [11] Richardson J.E. & Kedar S. (2013) *LPSC LPI Contribution No. 2863* [12] <https://isale-code.github.io/> [13] Teanby N.A. (2015) *Icarus* 256, 49-62. [14] Lundborg N. (1968) *Int. J. Rock Mech. Min. Sci.* 5: 427-454. [15] Pierazzo E. *et al.* (2005) *Spec. Pap., Geol. Soc. Am., vol. 384. GSA, Boulder, Colo.* 443–457. [16] Tillotson, J. H. (1962) *Technical report GA-3216, General Atomic Report*. [17] Wünnemann K. *et al.* (2006) *Icarus*, 180: 514-527. [18] Miljković, K. *et al.* (2012) *AIP Conf. Proc.* 1426, 871–874, doi:10.1063/1.3686416.